Microstructure - Mechanical Properties Relationships

In Inconel 706 Superalloy

G.W. Kuhlman*, A.K. Chakrabarti+, R.A. Beaumont*, E.D. Seaton*, J.F. Radavich++

* Alcoa Forged Products, Cleveland, Ohio;
+Alcoa Laboratories, Alcoa Center, Pa.;
++Micromet Laboratories, West Lafayette, Indiana

Abstract

The hot workability of Inconel Alloy 706 (IN 706) extends over a temperature range of 1700°F to 2100°F (925°C to 1150°C). The good hot workability of IN 706 in relatively large ingot sizes makes this alloy fabricable into large forgings utilized by important end markets including power generation, chemical processing, and others. Successful utilization of large IN 706 forgings in critical components requires control of important microstructural and mechanical property features. Grain size, grain boundary precipitates, and matrix precipitates vary widely in IN 706 as a result of fabrication history and post-fabrication thermal treatments (TMP). TMP conditions which favor heavy grain boundary precipitates, such as γ', γ'' and δ or η phases, affect ductility (elongation or reduction in area [RA]) and impact toughness (Charpy V-notch [CVN]) properties. Coarse matrix precipitates may also be observed. While tensile yield and ultimate strengths may increase slightly due to within grain and/or grain boundary precipitates, thicker, more continuous grain boundary precipitates result in lower ductility and toughness. Presented are fractographic and microscopic evaluations of IN 706 forgings illustrating key relationships between microstructure and ductility and fracture-related properties. Fracture behavior changes as grain interior and/or grain boundary precipitate and morphological features are changed. Critical impact properties of IN 706 are rationalized by microstructural observations.

Background

Inconel Alloy 706 (IN 706) is an important superalloy material for very large, commercial scale forgings utilized in several critical applications including power generation and chemical processing. Triple melted, VIM-ESR-VAR ingots, 32 to 36 in. (81 to 91 cm.) weighing over 30,000 lbs. (13,600 Kg.), are now routinely produced by several metal producers for fabrication into the large forgings specified for these applications. Casting of IN 706 ingots of this large size are feasible due the alloy's reduced propensity for segregation in comparison to Inconel Alloy 718. The composition and processing of the alloy provides excellent property combinations for highly stressed parts, including rotating components, in elevated temperature and/or corrosive environments. IN 706's reduced segregation potential may be linked to lower hardening element contents: 1) Nb - nominal 2.9% vs. 5.25% for IN 718 and (2) Al - 0.4% maximum vs. nominal 0.6% for IN 718. For adequate strength development, Ti content of IN 706 is higher than IN 718, e.g. nominal 1.75% vs.

Superalloys 718, 625, 706 and Various Derivatives
Edited by E.A. Loria
The Minerals, Metals & Materials Society, 1994

nominal 0.9% for IN 718.

In current major IN 706 applications, critical properties being captured are room and elevated temperature strengths, impact toughness, fatigue and ductility. A two-step heat treatment process, consisting of solution treatment, a liquid quench and a two-step age, which optimizes strength and fatigue performance is employed[1]. TMP for large IN 706 forgings has been under commercial development since the mid-1980's, leading to the successful processes now exploited on full scale forgings. Of significant concern in the design and execution of TMP for these very large parts is achieving acceptable grain size and microstructures, within the constraints and bounds of poor thermal conductivity, restricted heat transfer, and limitations on deformation processes and deformation history due to forging size, etc. typical of IN 706 in the very heavy section, large forged shapes being utilized. Deformation and process modeling has played a very important role in the forging engineering and process design and execution of large IN 706 parts.

Initially, understanding of microstructure-property relationships for IN 706 was based upon extensive work with its "parent" alloy, IN 718[2-4]. The fundamental building blocks of process-microstructure-properties interactions developed for IN 718 have been fully utilized in laying the foundation for the interpretation and understanding of IN 706 and its forging/thermal process development and capture. Recently, several workers[5-8] have contributed directly to the microstructural understanding of IN 706. The purpose of the within investigation for IN 706 is to provide further knowledge on structure-property relationships for this alloy in very large forged shapes.

Thermal treatment is a very important element of the TMP used for IN 706 and therefore final microstructures and properties. In review of structure-properties relationships for IN 706 and development of commercial thermal processes, the approximate T-T-T diagram[9] (Figure 1) is an important tool and has been extensively utilized as a guide in developing the critical thermomechanical processing (TMP) for IN 706. Improved understanding of phase relationships, improvements in the IN 706 T-T-T diagram and other key thermal and heat transfer properties of IN 706 are subjects of other papers at this Symposium.

For standardization purposes, phases and precipitates discussed herein are defined as follows:

(1) γ' - Gamma Prime - $Ni_3(Ti, Al)$, Face Centered Cubic (FCC)[5].
(2) γ'' - Gamma Double Prime - $Ni_3(Nb,Ti)$, Body Centered Tetragonal (BCT)[5]
(3) δ - Delta Phase - Ni_3Nb, Orthorhombic[6].
(4) η - Eta Phase - $Ni_3(Ti, Nb)$, Ordered Hexagonal Close-Packed (HCP)[6].

Procedures

This investigation was undertaken on a group of large IN 706 forgings fabricated under current specification criteria that include aggressive combinations of strength and toughness, the latter evaluated by Charpy V-Notch (CVN). The forgings involved have section thicknesses at the time of heat treatment from 12 to 17 in. (30 - 44 cm.) thick. Deformation and heat transfer (thermal treatment) modeling techniques were employed to develop and evaluate the forging process(es) and thermal treatment requirements in advance and to meet specification grain size and mechanical property objectives. From extensive testing of these heavy-section products, within any given forging or from forging-to-forging, a variation in mechanical properties,

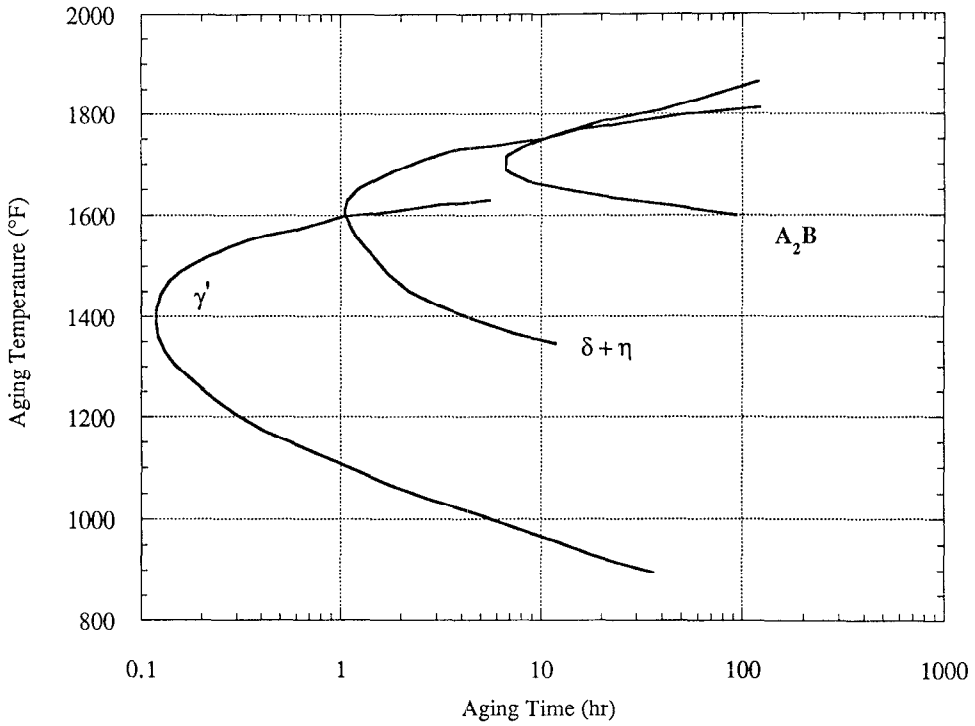

Figure 1: T-T-T Diagram for IN 706 Alloy With Silicon Content <0.07% Annealed @ 2000°F (1093°C) Followed by Aging @ Times Noted

specifically CVN, was frequently noted. In some instances CVN values were particularly low, leading to concern that the TMP practice may require optimization. Metallographic evaluations were undertaken to develop necessary understanding to guide processing revisions and to enhance impact toughness properties without degrading other important characteristics.

Table 1: Mechanical Properties Heavy Section IN 706 Forging.

Location	Dir	Yld. Str. Ksi (MPa)	Ult. Tens. Str. Ksi (MPa)	Elong %	RA %	CVN ft.-lbs. (joules)	ASTM Grain Size
Edge	L	155 [1068]	184 [1268]	21	39	49 [67]	4.1
Edge	T	151 [1041]	183 [1261]	19	36	45 [61]	4
Center	L	153 [1055]	178 [1227]	16	30	38 [52]	3.8
Center	T	151 [1041]	173 [1193]	16	29	26 [35]	3.9

One forging, nominally 14 in. (35 cm.) thick at the time of heat treatment, was selected for extensive fractographic and microstructural evaluation in order to better elucidate strength, ductility and CVN properties-microstructure relationships and if necessary, lead to modification of TMP to improve these properties. Table 1 presents the tensile strengths and ductilities, CVN and average ASTM grain size

properties measured at four locations within this part. Note that taken overall, yield and ultimate strengths and ductilities do not vary as much as CVN, e.g. the CVN at the center of the part is 40% lower than the CVN measured at the edge of the part, suggesting that quench rate and/or other thermal process phenomena may play an important role in defining critical microstructural features. Tensile and CVN specimens from these four locations were examined using SEM fractography and via SEM and TEM for microstructural observations. In addition, a few specimens were submitted for extraction followed by X-Ray diffraction and EDAX to identify specific phases present. Finally, a few critical specimens were also examined by TEM selected area diffraction to indentify phases presents. Microstructural observations were rationalized on the basis of the forging's working and thermal treatment histories and TMP vs. properties interactions to refine the processes for the forgings and improve toughness related properties.

Results and Discussion

Figures 2 and 3 present, respectively, the results of fractographic and high order SEM microscopy of the four test locations -- specimens evaluated being failed CVN test bars. Fractographically (Figure 2), the failure mode of CVN tested specimens changes as the CVN values increase. At low CVN's, the failure mode is virtually 100% intergranular, so much so, as in the case of the lowest CVN value, that the individual grains stand in relief (Figure 2, bottom). As CVN values increase, the fracture mode becomes more transgranular, such that at the highest CVN value in this group (upper micrograph, Figure 2), the fracture mode is about 80% transgranular. Examination of specimens from forgings with even higher CVN values, e.g. ≥ 70 ft.-lbs. (95 joules), the failure mode is virtually 100% transgranular. From the fractographs, fracture mode appears to be driven primarily by grain boundary phenomena and thus, the grain boundary phases and morphologies then are very important to impact (fracture) toughness of IN 706-STA forgings.

SEM microscopy presented in Figure 3 illustrates microstructures present at grain boundary and grain interiors of the four test specimens. In general the precipitate structures and morphologies of the grain interiors in these four specimens are similar, with relatively similar carbide levels and distributions and similar size and distributions of γ' and γ'', with the latter predominating[5,6]. Extraction and X-ray diffraction confirmed the predominate strengthening precipitate to be γ'/γ''. Higher strength specimens (upper two specimens in Figure 3) do have slightly finer matrix γ'/γ'' precipitates than the lower strength specimens in the bottom half of Figure 3.

Of most significance to CVN property differences noted in Table 1 and changes in failure mode in Figure 2, however, are the differences in grain boundary phases and morphologies when traversing Figure 3 from top to bottom, e.g. from high CVN values to low. The grain boundaries of the lower CVN values are heavily decorated with continuous or nearly-continuous, coarse phases, whereas for the higher CVN specimens (upper micrographs, Figure 3) grain boundary phases are discontinuous, serrated and fine. Extraction techniques along with selected area diffraction techniques have identified the predominate grain boundary phases as being γ'/γ'', carbides (MC, M_3C) and δ phase.

Selected area diffraction (SAD) was exploited to confirm phases and morphologies present at critical grain boundaries. Both γ' and γ'' precipitates are observed as is illustrated by the SAD observations in Figure 4. This figure shows the electron diffraction pattern of the lowest impact toughness specimen in Table 1 (CVN = 26 ft.-

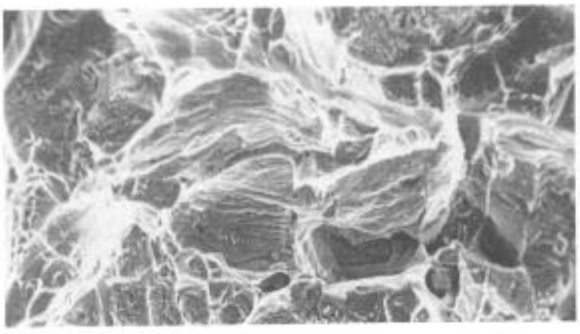

Fractograph, Inconel 706 - STA,
U.T.S. 184 Ksi (1268 MPa),
RA 39%
CVN: 49 ft.-lbs. (67 joules)
Average Grain Size ASTM 4.1
Magnification 300X

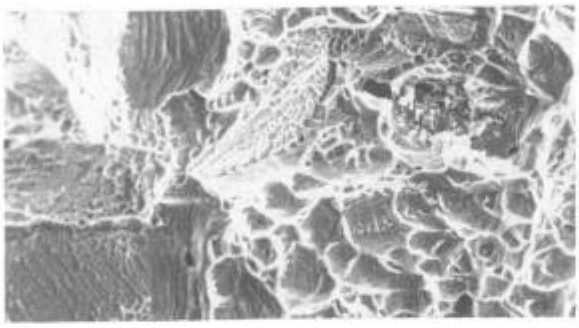

Fractograph, Inconel 706 - STA
U.T.S. 183 Ksi (1261 MPa)
RA 36%
CVN: 45 ft-lbs. (61 joules)
Average Grain Size ASTM 4.0
Magnification 300X

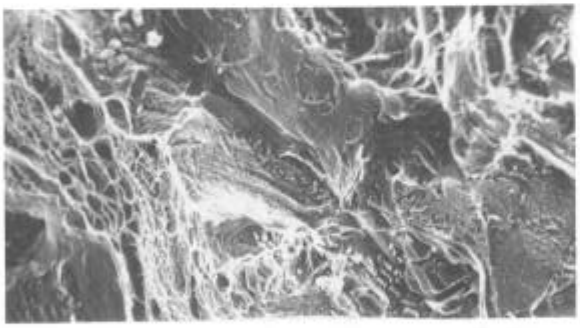

Fractograph, Inconel 706 - STA
U.T.S. 178 Ksi (1227 MPa),
RA 30%
CVN: 38 ft-lbs. (52 joules)
Average Grain Size ASTM 3.8
Magnification 300X

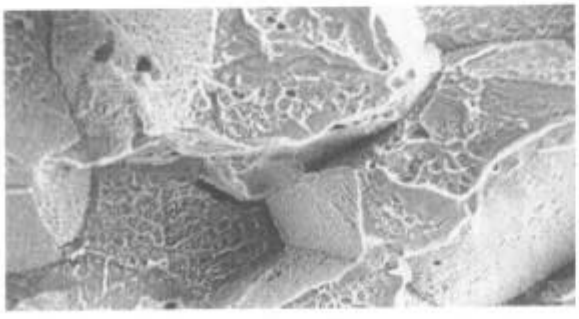

Fractograph, Inconel 706 - STA
U.T.S. 173 Ksi (1193 MPa)
RA 29%
CVN: 26 ft.-lbs. (36 joules)
Average Grain Size ASTM 3.8
Magnification 300X

Figure 2: Fractographic Evaluation, Inconel 706 - STA Forgings.

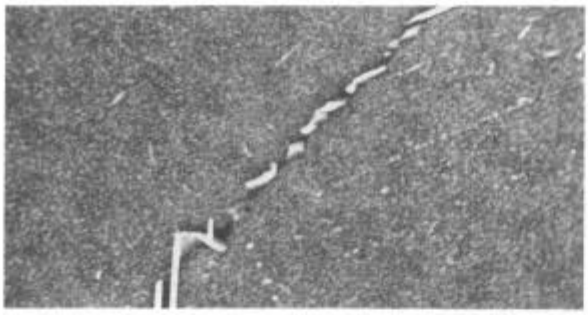

SEM Micrograph, Inconel 706 - STA,
U.T.S. 184 Ksi (1268 MPa),
RA 39%
CVN: 49 ft.-lbs. (67 joules)
Average Grain Size ASTM 4.1
Magnification 10,000X

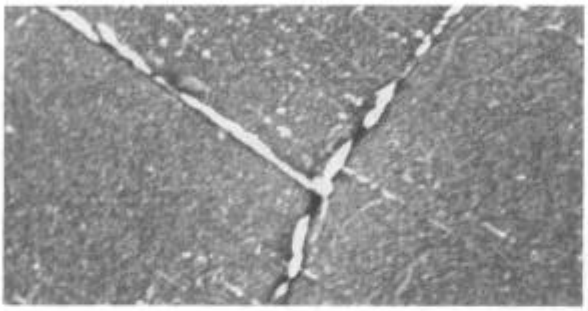

SEM Micrograph, Inconel 706 - STA
U.T.S. 183 Ksi (1261 MPa),
RA 36%
CVN: 45 ft-lbs. (61 joules)
Average Grain Size ASTM 4.0
Magnification 10,000X

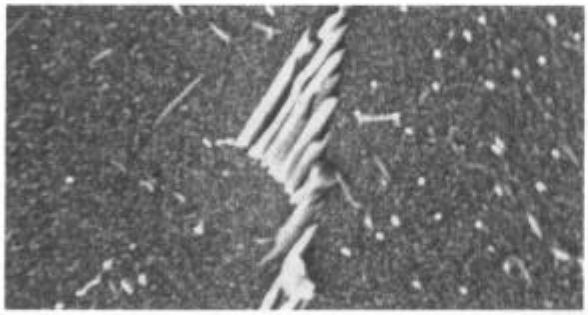

SEM Micrograph, Inconel 706 - STA
U.T.S. 178 Ksi (1227 MPa),
RA 30%
CVN: 38 ft-lbs. (52 joules)
Average Grain Size ASTM 3.8
Magnification 10,000X

SEM Micrograph, Inconel 706 - STA
U.T.S. 173 Ksi (1193 MPa),
RA 29%
CVN: 26 ft.-lbs. (36 joules)
Average Grain Size ASTM 3.9
Magnification 10,000X

Figure 3: SEM Metallographic Evaluation, Inconel 706 - STA Forgings.

lbs. [35 joules]) indicating the presence of γ''. Electron diffraction pattern of the same region as Figure 4, but tilted from z = <001> to z = <011>, Figure 5, shows the γ' and γ'' superlattice reflections.

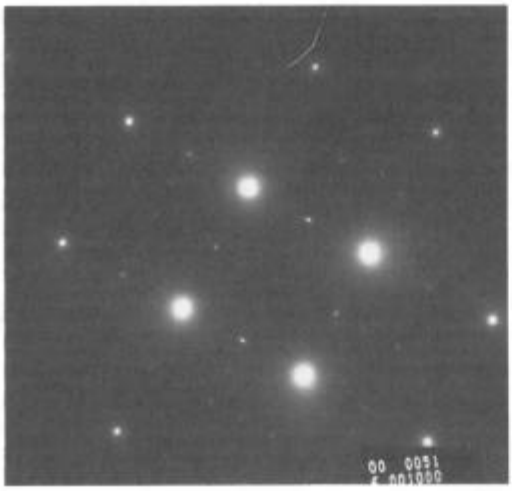

Figure 4: Electron Diffraction Pattern, Matrix Lowest CVN specimen Table 1, z = <001>, L = 903mm, 120kV.

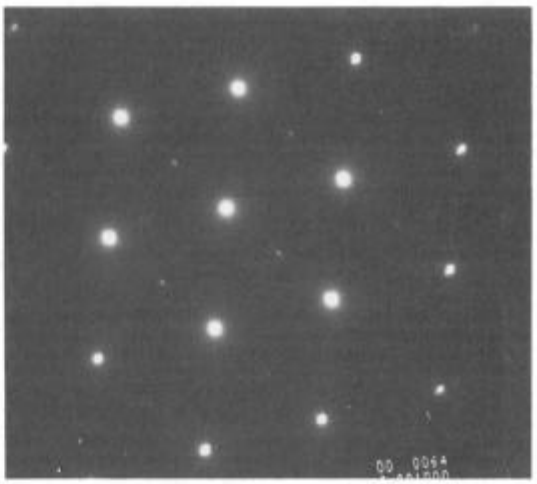

Figure 5: Electron Diffraction Pattern Same Region, Tilted from z = <001> to z = <011>. L = 903mm, 120kV.

Continuous type of grain boundary precipitates are also observed in SEM micrographs (Figure 3) for the low impact toughness specimen, Table 1, (CVN = 26 ft.-lbs. [35 joules]). Matching bright (left) and dark (right) field images of a continuous type grain boundary precipitate are shown in Figures 6A and 6B below presented

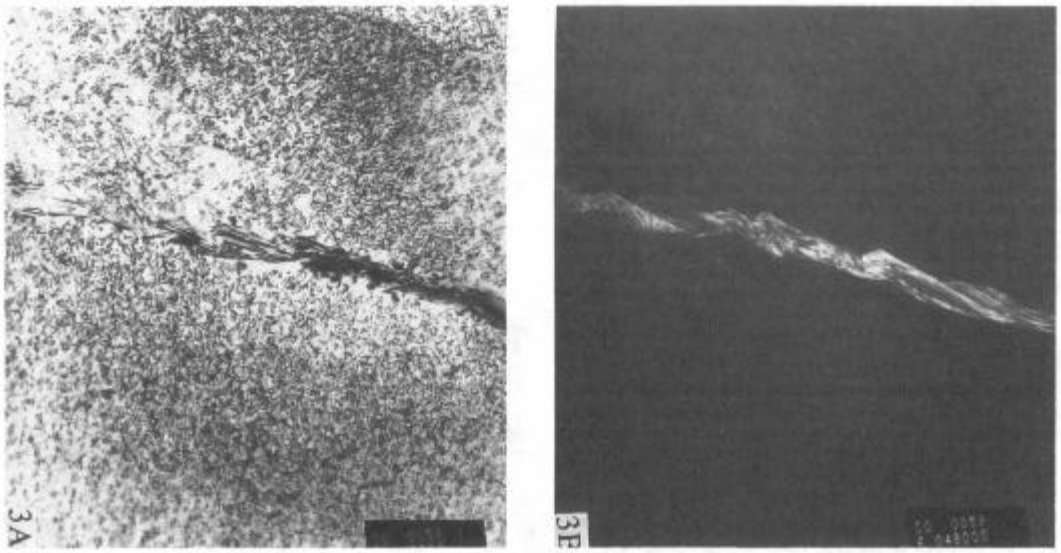

Figure 6: Matching Bright (3A) and Dark (3B) Field Images of a Continuous Type Grain Boundary Precipitate, Lowest CVN Specimen, Table 1. 48,000 X Magnification.

at 48,000 magnification. In further analysis of these specimens (Figure 6A/B) selected area diffraction patterns for this continuous type of grain boundary

precipitate are presented in Figures 7A and 7B. Superlattice ordering can be observed as dimmer spots in Figure 7B. The d-spacings calculated from this figure are shown in Table 2. From the SAD evaluation and calculated d-spacings, in

Table 2: Calculated d-Spacings from Figure 7 Compared to JCPDS.

d Spacing (Angstroms)	JCPDS 15-101 (δ)	JCPDS 5-723 (η)
4.56	-	-
3.22	3.26	-
2.29	2.27	-
2.23	2.23	2.21
1.75	1.81	1.72
1.61	-	-
1.57	1.55	1.54
1.53	1.54	1.51
1.17	-	1.17
1.14	1.13	-
1.11	1.11	1.1
0.874	-	-
a=5.11	b=4.25	c=4.56

particularly heavily decorated grain boundaries, such as illustrated here, and representative of the lowest observed CVN values from these heavy section IN 706 forgings, there is a significant amount of orthorhombic δ phase, with lesser amounts of the ordered η phase. From other specimens, there is either lesser amounts or the absence of these phases at grain boundaries with higher CVN values.

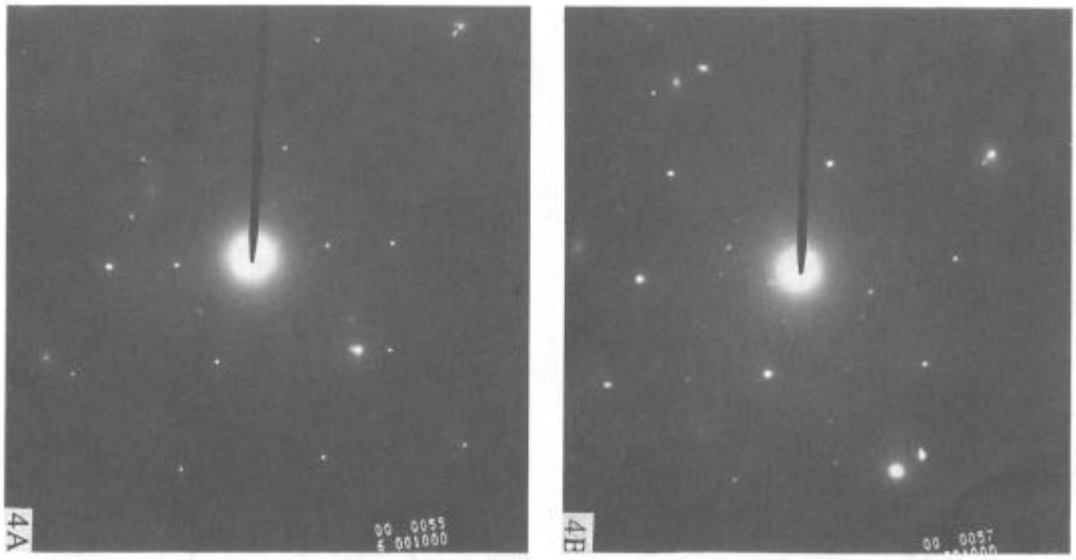

Figure 7: Selected Area Diffraction Pattern of the Continuous Type Grain Boundary Precipitate in Figure 6, Exhibits the Presence of δ Phase (4A), Superlattice Ordering of η Phase (4B), L = 903 mm, 120 kV.

From above analyses, control of grain boundary precipitates and morphologies is thus very important to enhancing the impact toughness of heat treated IN 706 forgings. Several processing factors in the fabrication stream of this alloy for heavy

section forgings may be involved, including (1) grain size from the forging deformation history, (2) cooling rates from thermal processes both forging and heat treatment and (3) final aging practices and resulting aging phenomena. From the T-T-T diagram (Figure 1) cooling rates in the several thermal processes required in the fabrication history of these large forgings, including solution heat treatment and/or forging preheating, must be considered as potential primary processes that can affect grain boundary precipitate and morphology conditions.

In the instance of the thick forging in question, the cooling rate at the center of the forging during heat treatment can be expected to be significantly slower than the edge of this same forging. From cooling rate studies of liquid quenching, the center of the heavy section IN 706 forging may cool at rates ≤25°F(14°C)/second, whereas the edge of the same forging may cool at rates ≥300°F(165°C)/sec. From the T-T-T diagram, fast cooling rates result in γ' and γ'' precipitation in aging whereas slower cooling rates, in the range of that encountered at the center of the forging, may result in aging entering the nose of the δ and η phase regions and precipitating these phases at boundaries.

In addition, acting either independently on grain boundary phenomena or as a adjunct to and in conjunction with prior thermal histories is the effect of the recommended two-step aging process (1350F [730°C]), 8 hrs., Fce. Cool @ 100°F [55°C]/hr. to 1150°F [620°C], 8 hrs. air cool) for optimum strength properties and its affect on grain boundary precipitate morphology. Aging practices for these heavy section parts are carefully designed and controlled to manage sluggish thermal conductivity and heavy section sizes. Thermomechanical processes have now been designed for large, heavy section IN 706 forgings that reduce grain boundary effects and routinely provide large forgings with longitudinal CVN values in excess of 50 - 60 ft.-lbs. (68 - 82 joules).

Conclusions

Fractographic, SEM, TEM, and Selected Area Diffraction evaluations of broken IN 706 CVN specimens removed from various locations within a heavy section forging displaying a range of impact values from 26 ft.-lbs. (35 joules) to 49 ft.-lbs. (67 joules) suggest:

(1) Fracture behavior transitions from predominately intergranular at lower CVN values to predominately transgranular at higher CVN values.

(2) The change in fracture behavior with CVN level appears associated primarily with changes in grain boundary precipitates and their morphology.

(3) The predominate matrix strengthening precipitates in IN 706 are BCT γ'' and FCC γ'. The size/distribution of the γ'/γ'' phase materially influences matrix tensile strength but not impact toughness (CVN).

(4) Heavily decorated, continuous, coarse grain boundary precipitates are typical of specimens with low CVN and intergranular fracture behavior. Sparsely decorated, discontinuous and/or serrated grain boundary precipitates are typical of specimens with high CVN and transgranular fracture behavior.

(5) Grain boundaries contain both γ' and γ'' precipitates but the coarser, more heavily decorated boundaries from low CVN specimens contain significant amounts of δ phase and lesser amounts of η phase.

(6) Grain boundary precipitates and their morphologies are heavily influenced by cooling rates during deformation history and/or during solution treatment. Post solution cooling rates in combination with aging process may lead to observed grain boundary precipitates and precipitate morphologies.

Acknowledgment

The authors wish to thank Mr. Karl A. Heck of INCO Alloys International for conducting the Selected Area Diffraction and TEM analyses.

References

1. Inconel Alloy 706, Inco Alloys International, 1974.
2. Muzyka, D.R., Maniar, G.N., "Effects of Solution Treating Temperature and Microstructure on the Properties of Hot Rolled 718 Alloy," Metals Engineering Quarterly, ASM International, November 1969, pp. 23 - 37.
3. Barker, J.F., Krueger, D.D., Change, D.R., "Thermomechanical Processing Of Inconel 718 and Its Effect on Properties,"
4. Mataya, M.C., Robinson, M.L., Chang, D., "Grain Refinement During Primary Breakdown of Alloy 718,"
5. Raymond, E.L., Wells, D.A., "Effects of Aluminum Content and Heat Treatment on Gamma Prime Structure and Yield Strength of Inconel Nickel-Chromium Alloy 706," Superalloy Processing, Proceedings of 2nd International Conference, MCIC Report, MCIC Battelle Columbus Laboratories, September 1972, pp. N-1 to N-21.
6. Remy, L., Laniesse, J. Aubert, H., "Precipitation Behavior and Creep Rupture of 706 Type Alloys," Materials Science and Engineering, 38, 1979, pp. 227-239.
7. Moll, J.H., Maniar, G.N., Muzyka, D.R., "Heat Treatment of 706 Alloy for Optimum 1200°F Stress-Rupture Properties," Metallurgical Transactions, Volume 2, August 1971, pp. 2153-2160.
8. Chkrabarti, A.K., Emptage, M.R., Kinnear, K.P., et.al., "Grain Refinement in IN 706 Disc Forgings Using Statistical Experimental Design and Analysis," Proceedings, 7th International Symposium on Superalloys, TMS, 1992, pp. 517-526.
9. Tamboo, S.V. , General Electric Power Systems Division, Private Communication.